Fast Fading Characterization for Body Area Networks in Circular Metallic Indoor Environments

FILIPE D. CARDOSO[1], **(Member, IEEE), PAWEŁ T. KOSZ**[2], **MANUEL M. FERREIRA**[1],
SŁAWOMIR J. AMBROZIAK[2], **(Senior Member, IEEE), AND**
LUIS M. CORREIA[3], **(Senior Member, IEEE)**

[1]ESTSetúbal, Polytechnic Institute of Setúbal and INESC-ID, 2914-508 Setúbal, Portugal
[2] Faculty of Electronics, Telecommunications and Informatics, Gdańsk University of Technology, 80-233 Gdańsk, Poland
[3]IST/INESC-ID, University of Lisbon, 1049-001 Lisbon, Portugal

Corresponding author: Filipe D. Cardoso (filipe.cardoso@estsetubal.ips.pt)

ABSTRACT With the increasing development of 5G and Body Area Network based systems being implemented in unusual environments, propagation inside metallic structures is a key aspect to characterize propagation effects inside ships and other similar environments, mostly composed of metallic walls. In this paper, indoor propagation inside circular metallic structures is addressed and fast fading statistical distributions parameters are obtained from simulation, being assessed with measurements at 2.45 GHz in a passenger ferry discotheque with an 8 m diameter circular shape. It is observed that, in this kind of environments, second order reflections are particularly relevant due to the walls' high reflective nature. Globally, it is concluded that the Rayleigh distribution can be used to characterize fast fading effects with no significant loss of accuracy compared to the Rice one, since a low value of the Rice parameter is observed, being below 3.1 dB, even under Line-of-Sight conditions. Moreover, it is observed that, from the fast fading viewpoint, the best transmitter position is at the circle center.

INDEX TERMS Body area networks, fading characterization, metallic structures, propagation modelling.

I. INTRODUCTION

The increasing number of applications of wireless technologies, the fast progress in miniaturization of electronic devices and the increasing demand for human health monitoring has directed the attention of researchers, system designers and application developers to Body Area Networks (BANs). These networks consist of small, lightweight, ultra-low-power short-range devices, which can be placed in, on, or around the human body in order to monitor different vital signals, exchange them between each other and send then to an external device [1].

There is also an interest of ships and passenger ferries owners in the implementation of BANs to increase the comfort and safety of passengers and employees during a cruise. Such networks will be able to monitor their vital signals, to enable localization features, and even to provide entertainment. The propagation environment of these networks should be

considered as a harsh and unusual environment, since walls, floors and ceilings are mostly made of metallic materials. Therefore, in order to ensure highly reliable radio links for the aforementioned applications, one has to thoroughly understand the propagation conditions in this type of scenarios and describe them by proper models.

There are various studies on propagation characteristics for BANs in different environments [2], [3], [4], especially for medical applications [5], [6]; most of them describe BAN measurements in typical, easily accessible, indoor environments, such as rooms [7], [8], corridors, hospital rooms, laboratories, or even in an anechoic chamber.

There is also a limited number of papers describing research on radio wave propagation in ship environments. A path loss model for a ship environment at 2.4 GHz has been proposed in [9], where two different ferries and three types of rooms, i.e. engine room, passengers' deck and vehicles parking, have been investigated. Other studies have been described in [10], where the characterization of the wireless channel at 2.5 GHz on board a cruise ship (hall and corridor)

The associate editor coordinating the review of this manuscript and approving it for publication was Theofanis P. Raptis.

has been presented. In [11], a wideband channel characterization along a lift shaft on board a ship at 255.6 MHz has been presented. The authors of [12] have performed an empirical study on board naval vessels, including path loss and delay spread in the range [0.8, 2.6] GHz at the machine and engine rooms and at a main starboard hallway. Finally, in [13], a complex electromagnetic environment characterization for two types of below-deck spaces in ships, i.e. an ordnance magazine and a pyrotechnics storage room, has been presented, for [0.1, 10] GHz. But all the above-mentioned studies for ship environments do not consider the specific aspects of BANs.

To the best of the authors' knowledge, the first research on BAN radio channels in metallic environment has been described in [14] and [15]. Measurements have been performed, allowing to establish empiric narrow- and ultra-wideband system loss and fading models at 0.868, 2.45 and 6.489 GHz, for a ferryboat environment [16], [17]; as a result it was established that slow fading is well modelled by the Lognormal Distribution while the Nakagami Distribution is best suited for modelling fast fading. Nevertheless, it is observed that the values of the Nakagami Distribution parameters for most cases change in a small range, which means that the power and fading depth are very similar for all scenarios, being close to the ones observed for the Rayleigh and Rice Distributions, since the value of Nakagami Distribution's m parameter is about 1.0, thus, corresponding to low values of the Rice Factor, K (the highest value is 1.0 dB.)

However, the above-mentioned studies have been done for corridors (with rectangular cross sections) and passengers' cabins, while the focus of this paper is a circular (cylinder and hemisphere structured) indoor environment, composed of metallic (almost perfect conducting) walls, which has different propagation conditions. Since this kind of environments has some particular characteristics, namely the high reflective nature of the walls and the circular geometry that lead to different zones where a different number of reflections is observed, propagation inside circular structures is addressed, therefore, paving the way to properly understand the radio channel in this kind of environments. By using a two-dimensional approach, propagation inside circular structures is studied and fast fading parameters are derived. Results from experimental measurements in a discotheque inside a ship were used to properly assess simulation results, and the use of Rayleigh and Rice Distributions for modelling fast fading is discussed. The novel aspect of this paper is a theoretical and empirical characterization of the radio channel in a circular metallic room, which is a propagation environment that has not been analyzed so far, to the best of authors' knowledge, especially for BAN applications.

This paper is organized as follows. Propagation inside circular metallic structures is addressed in Section II. Measurements inside a discotheque in a passenger ferry are presented in Section III. In Section IV, simulation results obtained from a channel simulator are presented and assessed with measurements. In Section V, a fading analysis is performed, and fast fading statistical distribution parameters are derived. Conclusions are drawn in Section VI.

II. PROPAGATION INSIDE CIRCULAR METALLIC STRUCTURES
In what follows, propagation inside a circle with perfect conducting boundaries is analyzed, aiming at characterizing the different situations regarding the observed number of reflections depending on the relative position of both transmitter and receiver inside the circular structure.

Propagation inside metallic structures is usually addressed in the context of waveguides, including resonant cavities theory [18]. In this kind of structures, their physical dimensions are usually of the order of the wavelength. The problem addressed in this paper is quite different, since for the frequency being considered, 2.45 GHz, the wavelength is 12.2 cm, which is quite small compared to the environment dimensions (several meters). Hence, free-space propagation together with specular reflection is considered.

Reflection inside structures with perfect conducting walls has some specificities resulting from the fact that the value of the reflection coefficient is (or close to) -1, thus, the power of the reflected components being of the same order of magnitude compared to LoS (Line-of-Sight) ones (the only difference being only due to the different path lengths); an increased dependence on the order of reflections (number of reflections of each reflected component) is then observed from the received signal behavior viewpoint. For a fixed transmitter (Tx) position the power at the receiver (Rx) at any given location can be simply evaluated as the sum of the LoS component plus the reflected ones.

The electric field at Rx when taking up to n_r order reflections (isotropic antennas being considered) is given by

$$E_{nRef} = \sum_{m=1}^{n_r} \sum_{n=1}^{R_m} \frac{\sqrt{30P_t}}{d_{mn}} \Gamma_{ref}^m e^{-j\frac{2\pi d_{mn}}{\lambda}}, \quad (1)$$

where:
- Γ_{ref}^m : reflection coefficient of the m-th reflection order;
- λ : wavelength;
- d_{mn} : path length of the n-th ray of the m-th reflection order;
- n_r : reflection order;
- P_t : Tx power;
- R_m : number of reflected rays.

corresponding to a power at the Rx of [19]

$$P_{r[dBW]} = 132.8 + 20\log\left(\left|E_{nRef[V/m]}\right|\right) - 20\log\left(f_{[Hz]}\right) \quad (2)$$

The case of reflections inside a circular structure of perfect conducting boundaries has been previously addressed in [20], [21]. For two points inside the circle, 1st order reflections can be calculated with an analytical straightforward process, but high order ones lead to a more complex formulation, hence, in this paper an iterative process is used.

One considers the Rx located at point $R(x_r, y_r)$ and the Tx at $T(x_t, 0)$, both inside a circle of radius r, Figure 1.
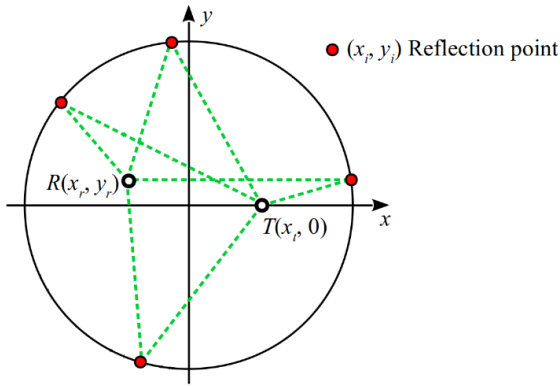
FIGURE 1. Reflections inside a circle.

When only 1st order reflections are considered, the reflection points can be evaluated as the roots x_i of the algebraic 4th order polynomial in y, given by [20]

$$y = \sum_{i=0}^{4} c_k x^i, \qquad (3)$$

with:

$$c_0 = vx_r^2 - vr^2 \left(1 + 2wx_r + w^2 x_r^2\right), \qquad (4a)$$

$$c_1 = 4vx_r + 2wvx_r^2 + 2w, \qquad (4b)$$

$$c_2 = v\left(1 + 2wx_r\right) + w^2 - 2u, \qquad (4c)$$

$$c_3 = -2u\left(vr + w\right), \qquad (4d)$$

$$c_4 = u^2, \qquad (4e)$$

where:

$$u = \frac{2}{r^2}, \qquad (5a)$$

$$v = \frac{1}{x_r^2 + y_r^2}, \qquad (5b)$$

$$w = \frac{1}{x_t}. \qquad (5c)$$

Reflection points (x_i, y_i) are then obtained from:

$$y_i = y_r \frac{2x_t x_i^2 - r^2 \left(x_i + x_t\right)}{2x_t x_r x_i - r^2 \left(x_r + x_t\right)}. \qquad (6)$$

where x_i are the roots of (3).

The influence of the position of Rx and Tx on the number of existing reflection points inside the circle is illustrated in Figure 2. The Rx and Tx relative position has a major influence on the number of reflections. The roots of (3) may be four real numbers, which results in four rays reflections, Figure 2a, or a pair of real solutions and a pair of complex ones, which results in two rays reflections, Figure 2b. As described in [20], regions with a different number of reflections are defined by catacaustic ones.

Figure 3 shows the catacaustic regions for different Tx positions, when only 1st order reflections are considered. The existence of these different areas implies a different behavior for the signal at the Rx, which poses significant challenges to fast fading characterization.
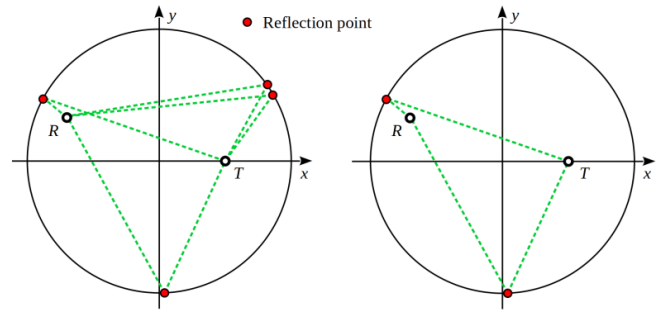

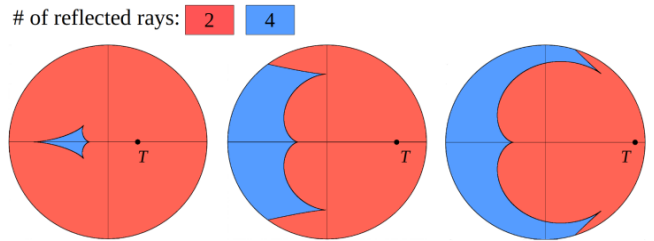**FIGURE 2.** Influence of Rx and Tx relative position on the number of reflections.

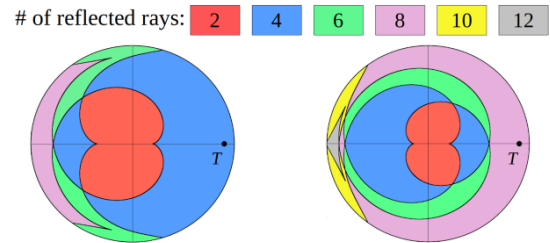**FIGURE 3.** Catacaustic regions for 1st order reflections.

FIGURE 4. Catacaustic regions for 2nd and 3rd order reflections.

Catacaustic regions for 2nd and 3rd order reflections are shown in Figure 4, for $T(0.9r, 0)$. For the 2nd order, different areas are observed corresponding to 2, 4, 6 or 8 reflected rays, while for the 3rd order, there are up to 12 reflected rays.

III. MEASUREMENT RESULTS
A. MEASUREMENT ENVIRONMENT, SCENARIO AND EQUIPMENT

The measurement campaign was carried out in a discotheque, located on the eighth deck of the passenger ferry M/F Wawel, during one of the cruises. The discotheque is an indoor environment with circular shape (with a diameter of 16 m) and hemispherical ceiling (with a height of 7.3 m), both the walls and the ceiling being metallic.

The campaign focused on system loss measurements in the link between a Tx antenna located on a human body (a man with 1.7 m height and 60 kg weight) in three locations (head's right side (HE_R), torso's front side (TO_F), and arm's left side (AB_L)) and an Rx antenna positioned off-body, Figure 5.

During measurements, due to the discotheque dimensions and to typical situations occurring for BANs in off-body communications, two walking scenarios have been considered: approaching and departing. These scenarios allow to
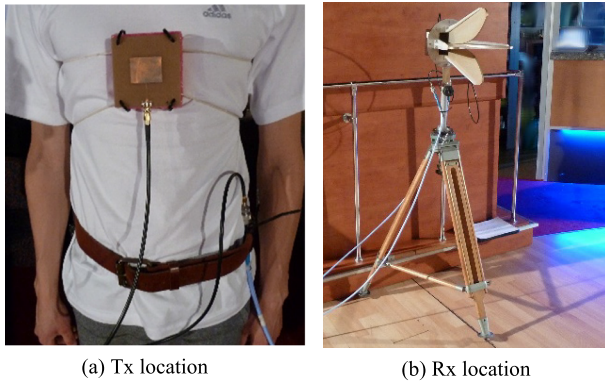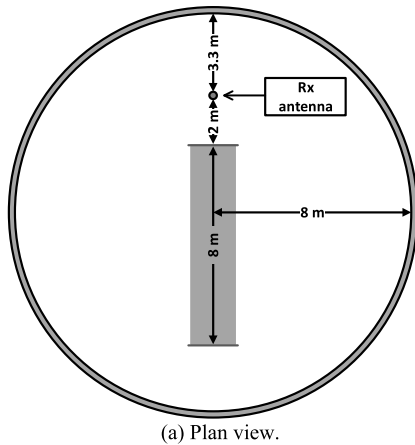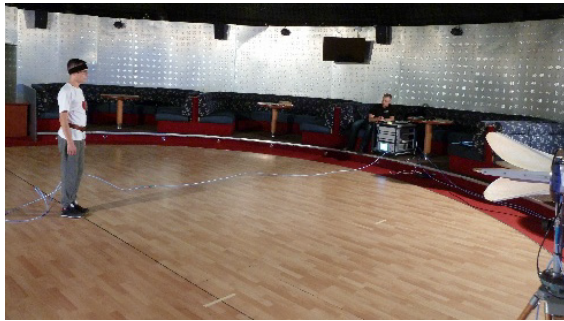
(a) Tx location   (b) Rx location

FIGURE 5. Transmitting and receiving antennas positioning.

(a) Plan view.

(b) Photo of a location.

FIGURE 6. View of the discotheque with the measurement area and Rx location.

perform the analysis of system loss for various conditions and on-body antenna placements. The distance between Tx and Rx varied from 2 to 10 m. For each Tx antenna configuration and walking scenario, measurements were repeated 10 times. Figure 6 shows the plan view of the discotheque with the measurement area and Rx location, and a photo of a location.

The considered scenarios and Tx on-body antenna placements allow, with respect to the orientation-dependent body shadowing, to investigate the three propagation conditions: LoS – when the Tx antenna is directed towards the Rx one; NLoS (Non-LoS) – when the Tx antenna is pointing away from the Rx one and the body fully obstructs the direct propagation path; and QLoS (Quasi-LoS) – when the Tx antenna is oriented orthogonally to the Rx one and the direct

TABLE 1. Fitting of measured fast fading distributions.

			PDF's parameters			
			Rice			Rayleigh
LoS	**Scenario**	**Tx**	s_{Ri}	σ_{Ri}	K [dB]	σ_{Ra}
LoS	Approaching	TO_F	0.98	0.53	2.3	0.87
QLoS	Approaching	HE_R	0.02	1.00	-37.0	1.00
		AB_L	0.65	0.86	-5.4	0.97
	Departing	HE_R	0.07	1.04	-26.4	1.04
		AB_L	0.03	1.00	-33.5	1.00
NLoS	Departing	TO_F	0.08	0.98	-24.8	0.98

propagation path is either clear or partially shadowed by the body.

The equipment described in [22] was used, configured for system loss measurements with polarization diversity. The measurements were performed in the ISM (Industrial, Scientific and Medical) band, centered at 2.45 GHz.

The Tx antenna was a wearable patch antenna, Figure 5a, with linear polarization, being characterized by a 3 dBi gain, and half-power beamwidths of 140° and 115° in the E- and H-planes, respectively. The transmitted signal was BPSK (*Binary Phase Shift Keying*) modulated by a pseudo-random bit sequence with a length of 23 bits at 3 kbit/s. After calibration, the signal power at the input of the Tx antenna was −4.2 dBm.

The Rx antenna was a dual polarized quad-ridged horn, Figure 5b, LB-OSJ-0760 [23], with a 10 dBi gain and half-power beamwidths of 58° and 46° in the E- and H-planes, respectively, mounted on a 1.3 m height tripod. The received power was evaluated at the RF level, hence, being independent of the modulation being used.

B. MEASUREMENT RESULTS

Since system loss and slow fading were addressed in [16], one focus on the fast fading characteristics, being assumed that they can be modelled by Rayleigh or Rice Distributions, since in the context of BANs, propagation paths are usually composed of a mixture of LoS and NLoS situations.

The fast fading behavior was extracted from measurement data and the obtained distributions were fitted to commonly used Probability Density Functions (PDFs) [24], using Maximum Likelihood Estimation (MLE) [26], implemented in Matlab®. Fast fading extraction was implemented as follows:

1. The slow fading signal was evaluated by averaging the measured values over a 10λ sliding window with a λ/2 displacement between consecutive samples.
2. The mean system loss was then evaluated from the linear regression of the slow fading signal.
3. Fast fading was obtained as the difference between the measured values of system loss and the slow fading signal.

Table 1 presents the results of the measured fast fading distributions fitting to the following PDFs:

- Rayleigh, with scale parameter σ_{Ra};

- Rice, with parameters, s_{Ri}, and, σ_{Ri} corresponding to the magnitude of the direct and reflected components, respectively.

The fitted PDFs passed the selected Goodness of Fit tests of correlation, chi-square and Akaike Information Criterion, which were considered for the validation of the considered distributions.

The value of K for LoS is 2.3 dB while for QLoS it ranges from -37.0 to -5.4 dB, the higher value being observed for Approaching/AB_L, because during walking the natural arm motion causes a change in the visibility of the antennas from LoS to QLoS, while for NLoS (the direct ray is obstructed by the body) it is -24.8 dB. Globally, K is lower than 2.3 dB, which is not surprising, due to the wall's high reflective nature (considered as perfect reflectors), hence, the power of the reflected rays being of the same order of magnitude of the direct one even for high order reflections.

IV. FAST FADING DEPENDENCE ON THE ORDER OF REFLECTIONS BEING CONSIDERED

In order to evaluate the dependence of fast fading on the reflections order, a two-dimensional simulator was implemented in Matlab®, allowing to properly evaluate the power at the Rx at any given location inside the circle with perfect conducting boundaries, as defined in Section II.

It should be stressed that in a real scenario walls are not perfect conducting boundaries and imperfections exist, having impact on the values of the reflection coefficient. Moreover, among other aspects, the scenario dynamics, namely due to the presence of people and obstacles, the use of different types of antennas/polarizations and the user body movement (causing antennas misalignment), will have quite an impact on results. Under the scope of the current work, the objective is to keep the model as simple as possible, while still being accurate enough to describe reality and keeping the deviation from measurements within an acceptable margin. Moreover, this is not a deterministic problem, therefore, all modeling approaches need to be of a statistical nature. Further enhancements to the model, allowing to address some of the issues already pointed out, and its assessment through measurements, will be implemented as soon as new measurement campaigns are performed.

Simulations were made for reflections order ranging from the 1st up to the 5th. A circle with radius $r = 8$ m was considered and the frequency was set to 2.45 GHz, corresponding to the measurement scenario described in Section III. The Tx and the Rx were randomly positioned inside the circle and the process was repeated 6 000 times.

Fast fading parameters were extracted from fitting simulation data to Rayleigh and Rice Distributions using MLE. Simulation results are presented in Table 2, with a varying reflection order n_r, meaning that reflections were considered for evaluating the power at the Rx up to the n_r order.

One can conclude that K ranges from -12.1 to 2.9 dB, the higher the order of reflections being considered the lower

TABLE 2. Statistical fading distribution parameters when considering from the 1st up to the 5th order reflections, LoS.

PDF	Parameter	Reflection order, n_r				
		1	2	3	4	5
Rayleigh	σ_{Ra}	0.84	0.86	0.88	0.89	0.89
Rice	s_{Ri}	0.97	0.92	0.85	0.53	0.29
	σ_{Ri}	0.49	0.57	0.64	0.76	0.83
	K [dB]	2.9	1.1	-0.5	-6.1	-12.1

TABLE 3. Statistical fading distribution parameters for 1st up to 5th order reflections, NLoS.

PDF	Parameter	Reflection order, n_r				
		1	2	3	4	5
Rayleigh	σ_{Ra}	0.85	0.89	0.91	0.93	0.93
Rice	s_{Ri}	0.87	0.04	0.03	0.03	0.03
	σ_{Ri}	0.59	0.89	0.91	0.93	0.93
	K [dB]	0.4	-30.0	-32.6	-32.8	-32.8

being the value of K, given that the power of the reflected components will increase correspondingly.

Under NLoS, i.e., without considering the direct path (ray) between Tx and Rx, the results are presented in Table 3.

As expected, one can conclude that K is below the one for the LoS case, ranging from -32.8 to 0.4 dB.

When comparing the simulated results with the measured ones for LoS, the measured value is between the simulated ones obtained for $n_r = 1$ and $n_r = 2$. For NLoS, the measured value of K is close to the simulated one for $n_r = 2$. The difference between the measured and simulated values of K is 5.2 dB, nevertheless, being of the order of -25 to -30 dB in both cases, i.e., from the statistical fading distribution viewpoint, no significant difference is observed.

Additionally, one should consider that in the measurement scenario directive antennas were used at both Tx and Rx, hence, the lower the reflected power the higher the value of K.

Globally, one concludes that in this kind of environments 2nd order reflections play an important role, which is not surprising due to the high reflective nature of the walls. It should be stressed that the real environment is not a two-dimensional one as assumed in the simulation model, but rather a three-dimensional indoor one, composed of a cylinder (walls) and a hemisphere (ceiling); nevertheless, fast fading effects in this kind of environments can be modelled with reasonable accuracy with the proposed model by considering up to 2nd order reflections. As previously, referred, the aim of the model is to keep it as simple as possible, while ensuring enough accuracy for radio channel and system analyses.

An example of the mapping between measurement and simulation results is illustrated in Figure 7. Simulation results were obtained for a scenario as the one depicted in Figure 6a, in order to replicate measurement conditions; the measurement correspond to the TO_F approaching LoS situation. It should be noted that, in the whole measurement campaign, this was the only situation where LoS exists during the whole path, which is why no additional comparisons are made. Globally, a good matching is observed: it is interesting to note that, in both simulation and measurement results, the two and
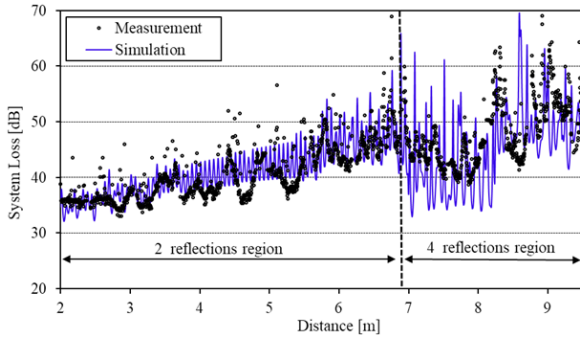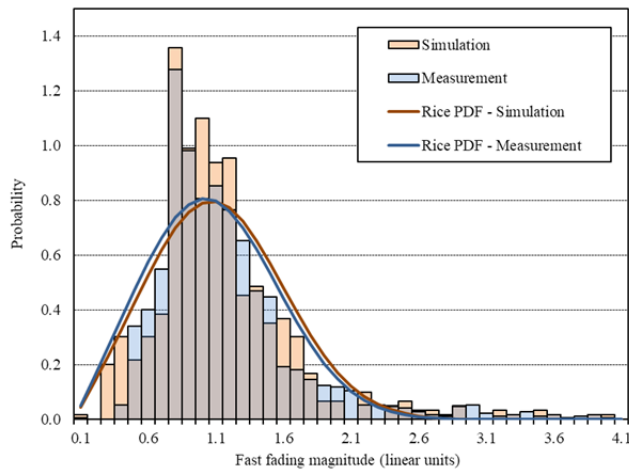
FIGURE 7. Measurement and simulation results.

FIGURE 8. PDF of measured and simulated results.

TABLE 4. Statistical fading distribution parameters, for the 2 reflections catacaustic region, LoS.

	Rice			Rayleigh
r/λ	s_{Ri}	σ_{Ri}	K [dB]	σ_{Ra}
33	0.96	0.52	2.3	0.85
49	0.96	0.50	2.7	0.85
66	0.96	0.50	2.7	0.84
82	0.96	0.49	2.8	0.84
98	0.97	0.48	3.1	0.83

TABLE 5. Statistical fading distribution parameters, for the 4 reflections catacaustic region, LoS.

	Rice			Rayleigh
r/λ	s_{Ri}	σ_{Ri}	K [dB]	σ_{Ra}
33	0.86	0.63	-0.3	0.88
49	0.89	0.60	0.4	0.87
66	0.90	0.59	0.7	0.87
82	0.92	0.57	1.1	0.86
98	0.93	0.55	1.6	0.85

TABLE 6. Statistical fading distribution parameters, for the 2 reflections catacaustic region, NLoS.

	Rice			Rayleigh
r/λ	s_{Ri}	σ_{Ri}	K [dB]	σ_{Ra}
33	0.08	0.94	-24.4	0.91
49	0.07	0.91	-25.3	0.88
66	0.04	0.91	-30.1	0.88
82	0.05	0.89	-28.0	0.86
98	0.04	0.89	-30.0	0.86

four reflections catacaustic regions can be clearly identified. A comparison between the obtained PDFs is done in II. The value of K, evaluated from the fitted PDF distributions, is 0.7 and 1.2 dB for measurements and simulations, respectively, being close to the ones obtained for the whole set of 10 measurement runs performed in this scenario (Table 1, TO_F, Approaching).

One should keep in mind that, as previously referred, several system and scenario aspects are not considered in the simulation model, nevertheless, besides not being exhaustively assessed with measurements, the proposed model provides a good fit with measurement results for the LoS case. Results for the QLoS and NLoS cases are not presented, still, a good matching is observed, with the received signal being well modelled by the Rayleigh distribution, as expected.

V. FADING ANALYSIS

The results in Section IV were derived for the whole circle (with $r = 8$ m) corresponding to the measurement scenario. In this section, one analyses fast fading in different catacaustic regions, as detailed in Section II, for different values of r/λ, in order to properly characterize propagation in these areas and for different radius. Simulations were made considering up to 2nd order reflections and r/λ equal to 33, 49, 66, 82 and 98, roughly corresponding to a radius of 4, 6, 8, 10 and 12 m, respectively, for the frequency being considered.

As previously, Tx and Rx were randomly positioned inside the circle and the process was repeated 6 000 times. For each Tx location, the catacaustic region is identified, allowing to evaluate the statistics for the different cases; when referring to 2 and 4 reflections catacaustic regions one means the regions where only 1st order reflections are considered.

Results for LoS in the 2 reflections catacaustic region are presented in Table 4. K ranges from 2.3 to 3.1 dB, slightly increasing for increasing values of r/λ, the difference between $r/\lambda = 33$ and $r/\lambda = 98$ being 0.8 dB.

Results for the 4 reflections catacaustic region are presented in Table 5. K ranges from -0.3 to 1.6 dB, being lower compared to the 2 reflections catacaustic region. On average, K is between 1.5 and 2.6 dB, below the one observed for the 2 reflections case, with the difference increasing almost linearly with decreasing values of r/λ.

When one focus on the fading margin required for coverage planning purposes, it is concluded that, besides being an LoS situation, the Rayleigh Distribution can be used for modelling fast fading with a reasonable accuracy, since the difference in the fading margin obtained from the Rice Distribution with $K = 3.1$ dB (the higher value of K being observed) and the one obtained from the Rayleigh distribution is 2.4 dB (for 95% coverage probability).

Results for NLoS and 2 and 4 reflections catacaustic regions, respectively, are presented in Table 6 and Table 7.

TABLE 7. Statistical fading distribution parameters, for the 4 reflections catacaustic region, NLoS.

	Rice			Rayleigh
r/λ	s_{Ri}	σ_{Ri}	K [dB]	σ_{Ra}
33	0.05	0.95	-28.6	0.95
49	0.05	0.91	-28.2	0.91
66	0.04	0.90	-30.1	0.90
82	0.04	0.88	-29.9	0.88
98	0.04	0.87	-29.8	0.87

From Table 6, one concludes that K ranges from -30.1 to -24.4 dB, with a small tendency to decrease for increasing values of r/λ. The results for the 4 reflections catacaustic region are slightly below the ones for the 2 reflections catacaustic one, still no significant difference on the value of K being observed in both catacaustic regions.

It should be stressed that the values of K observed in NLoS should be considered only as being illustrative of the small values of K obtained in these conditions, rather than its absolute value itself. It is well known that for $K \leq -3$ dB the PDFs of the Rice Distribution are practically superimposed, coinciding with the Rayleigh one, hence, a low accuracy on the evaluation of K, obtained from the fitted Rice Distribution parameters is observed.

Taking into account that the size of the 4 reflections catacaustic region, the one in which more severe fading is usually observed, decreases with the decreasing distance between the Tx and the circle center (Figure 3), the closer the Tx is to the circle center the smaller is the 4 reflections zone, hence, the lower the probability of a Rx being there experiencing a lower value of K (associated to a lower fading margin). One should note that, as previously referred, for both LoS and NLoS, fast fading is reasonably modelled by a Rayleigh Distribution, hence, no significant differences in fading margin in different catacaustic regions are observed. Nevertheless, by positioning the Tx in the circle center one ensures that there is only one catacaustic region (the 2 reflections one), where higher values of K are obtained.

VI. CONCLUSION

In this paper, propagation inside circular metallic structures is addressed and a model is developed and assessed with measurements in a passenger ferry cylindrical discotheque allowing to derive fast fading statistical distributions parameters.

It is observed that, in this kind of environments, 2nd order reflections are significant due to the walls' high reflective nature. Globally, it is concluded that the Rayleigh Distribution can be used to characterize fast fading, with no significant loss of accuracy compared to the Rice Distribution, since a low value of the Rice parameter, K, is usually observed for the scenarios being considered, being between -30.1 and 3.1 dB. Moreover, since in a BAN environment the LoS path will be continuously "on" and "off" due to body movement, it is expected that in a real mobility scenario the average value of K will be well below 3.1 dB.

In a worst case scenario, from the viewpoint of the Rayleigh Distribution applicability to model fast fading, if one refers to the fading margin required in this kind of environments, the difference in this margin for a 95% coverage probability, when considering a Rayleigh Distribution or a Rice one with $K = 3.1$ dB, is approximately 2.4 dB regarding the median value. From the cellular planning viewpoint, it is observed that the best Tx position in order to provide a uniform coverage of the whole area is at the circle center. This is not surprising from the link budget viewpoint, still, the same conclusion is not straightforward when referring to fast fading, as presented in this paper.

In conclusion, fast fading can be well modelled by a Rayleigh Distribution, with no significant loss of accuracy, even for LoS, with no need of using more complex distributions. This paves the way for a simple coverage planning in cylindrical and hemispherical structures as usually found in such specific environments.

Further work includes additional measurement campaigns and study in order to evaluate the influence of system and scenario specific issues, namely, walls characteristics, scenario dynamics, use of different types of antennas with different polarizations and user body movement, on the fading distribution being used for characterizing fading effects.

REFERENCES

[1] A. Reichman and J. Takada, "Body communications," in *Pervasive Mobile and Ambient Wireless Communications*, R. Verdone and A. Zanella, Eds. London, U.K.: Springer, 2012.

[2] *Channel Model for Body Area Network*, IEEE Standard P802.15, Working Group for Wireless Personal Area Networks, New York, NY, USA, 2009.

[3] D. B. Smith, D. Miniutti, T. A. Lamahewa, and L. W. Hanlen, "Propagation models for body-area networks: A survey and new outlook," *IEEE Antennas Propag. Mag.*, vol. 55, no. 5, pp. 97–117, Oct. 2013.

[4] S. J. Ambroziak, L. M. Correia, and K. Turbic, "Radio channel measurements in body-to-body communications in different scenarios," in *Proc. URSI Asia–Pacific Radio Sci. Conf. (URSI AP-RASC)*, Seoul, South Korea, Aug. 2016, pp. 1376–1379.

[5] P. A. Catherwood and W. G. Scanlon, "Link characteristics for an off-body UWB transmitter in a hospital environment," in *Proc. Loughborough Antennas Propag. Conf.*, Loughborough, U.K., Nov. 2009, pp. 569–572.

[6] P.-F. Cui, Y. Yu, W.-J. Lu, Y. Liu, and H.-B. Zhu, "Measurement and modeling of wireless off-body propagation characteristics under hospital environment at 6–8.5 GHz," *IEEE Access*, vol. 5, pp. 10915–10923, May 2017.

[7] L. Xia, S. Redfield, and P. Chiang, "Experimental characterization of a UWB channel for body area networks," *EURASIP J. Wireless Commun. Netw.*, vol. 2011, no. 1, Jan. 2011.

[8] S. J. Ambroziak, L. M. Correia, R. J. Katulski, M. Mackowiak, C. Oliveira, J. Sadowski, and K. Turbic, "An off-body channel model for body area networks in indoor environments," *IEEE Trans. Antennas Propag.*, vol. 64, no. 9, pp. 4022–4035, Sep. 2016.

[9] H. Kdouh, C. Brousseau, G. Zaharia, G. Grunfelder, and G. E. Zein, "Measurements and path loss models for shipboard environments at 2.4 GHz," in *Proc. 41st Eur. Microw. Conf.*, Manchester, U.K., Oct. 2011, pp. 408–411.

[10] A. Mariscotti, M. Sassi, A. Qualizza, and M. Lenardon, "On the propagation of wireless signals on board ships," in *Proc. IEEE Instrum. Meas. Technol. Conf.*, Austin, TX, USA, May 2010, pp. 1418–1423.

[11] X. H. Mao, Y. H. Lee, and B. C. Ng, "Wideband channel characterization along a lift shaft on board a ship," in *Proc. IEEE Antennas Propag. Soc. Int. Symp.*, Toronto, ON, Canada, Jul. 2010, pp. 1–4.

[12] E. Balboni, J. Ford, R. Tingley, K. Toomey, and J. Vytal, "An empirical study of radio propagation aboard naval vessels," in *Proc. IEEE-APS Conf. Antennas Propag. Wireless Commun.*, Waltham, MA, USA, Nov. 2000, pp. 157–160.

[13] G. B. Tait and M. B. Slocum, "Electromagnetic environment characterization of below-deck spaces in ships," in *Proc. IEEE Int. Symp. Electromagn. Compat.*, Detroit, MI, USA, Aug. 2008, pp. 1–6.

[14] K. K. Cwalina, S. J. Ambroziak, P. Rajchowski, and L. M. Correia, "Radio channel measurements in 868 MHz off-body communications in a ferry environment," in *Proc. 32nd Gen. Assem. Sci. Symp. Int. Union Radio Sci. (URSI GASS)*, Montreal, QC, Canada, Aug. 2017, pp. 1–4.

[15] P. T. Kosz, S. J. Ambroziak, and L. M. Correia, "Radio channel measurements in off-body communications in a ferry passenger cabin," in *Proc. 32nd Gen. Assem. Sci. Symp. Int. Union Radio Sci. (URSI GASS)*, Montreal, QC, Canada, Aug. 2017, pp. 1–4.

[16] P. T. Kosz, S. J. Ambroziak, J. Stefanski, K. K. Cwalina, L. M. Correia, and K. Turbic, "An empirical system loss model for body area networks in a passenger ferry environment," in *Proc. Baltic URSI Symp. (URSI)*, Poznan, Poland, May 2018, pp. 57–60.

[17] K. Cwalina, S. Ambroziak, and P. Rajchowski, "An off-body narrowband and ultra-wide band channel model for body area networks in a ferryboat environment," *Appl. Sci.*, vol. 8, no. 6, p. 988, Jun. 2018.

[18] A. Weisshaar, G. C. Alexander, P. C. Magnusson, and V. K. Tripathi, *Transmission Lines and Wave Propagation*. Boca Raton, FL, USA: CRC Press, 2000.

[19] J. D. Parsons, *The Mobile Radio Propagation Channel*. Chichester, U.K.: Wiley, 2000.

[20] G. Glaeser, "Reflections on spheres and cylinders of revolution," *J. Geometry Graph.*, vol. 3, no. 2, pp. 121–139, 1999.

[21] E. H. Lockwood, *A Book of Curves*. Cambridge, U.K.: Cambridge Univ. Press, 1961.

[22] S. J. Ambroziak, "Measurement stand and methodology for research of the off-body and Body-to-Body radio channels in WBANs with different diversity schemes," *Int. J. Antennas Propag.*, vol. 2019, pp. 1–16, Apr. 2019.

[23] (Jul. 2019). *A-Info, LB-OSJ-0760 Dual Polarised Quad-Ridged Horn Antenna*. [Online]. Available: http://www.ainfoinc.com/en/pro_pdf/new_products/antenna/Dual%20Polarization%20Horn%20Antenna/tr_LB-OSJ-0760.pdf

[24] G. L. Stüber, *Principles of Mobile Communication*, 2nd ed. Dordrecht, The Netherlands: Academic, 2002.

[25] H. Cramér, *Mathematical Methods of Statistics*. Princeton, NJ, USA: Princeton Univ. Press, 1999.

[26] L. Lauwers, K. Barbe, W. Van Moer, and R. Pintelon, "Estimating the parameters of a rice distribution: A Bayesian approach," in *Proc. IEEE Intrumentation Meas. Technol. Conf.*, Singapore, May 2009, pp. 114–117.

PAWEŁ T. KOSZ was born in Poland, in 1991. He received the Eng. and M.Sc. degrees in radio communication from the Gdańsk University of Technology (GUT), Poland, in 2014 and 2015, respectively. Since 2015, he has been with the Radio Communication Systems and Networks Department (GUT) as Ph.D. student of telecommunication, and also as an IT Specialist employee, until 2019. He has participated in European COST Action (CA15104) - IRACON. His research interests are concerned with propagation of radio waves in indoor environments and wireless body area networks. He was a recipient of the Best Paper Award for Master Thesis in 2016 funded by the Polish Association of Telecommunication Engineers, and the Young Scientists Awards of URSI in Best Paper competition, in 2017.

MANUEL M. FERREIRA received the Licenciado degree in electronics and telecommunications from the University of Aveiro and the M.Sc. degree in electrical and computer engineering from the IST/Technical University of Lisbon. Since 1995, he has been with the Department of Electrical Engineering, ESTSetúbal/Polytechnic Institute of Setúbal, Portugal. He was involved in European projects and networks of excellence NEWCOM and ICT/LEXNET. His research interests include wireless/mobile channel characterization and wireless sensor networks.

FILIPE D. CARDOSO (Member, IEEE) received the Licenciado, M.Sc., and Ph.D. degrees in electrical and computer engineering from the IST/Technical University of Lisbon. Since 1994, he has been with the Department of Electrical Engineering, ESTSetúbal/Polytechnic Institute of Setúbal, Portugal, where he is currently a Tenured Professor in telecommunications and also the Head of the Electronics and Telecommunications area. He is a Researcher with INESC-ID, Lisbon. His research interest includes wireless/mobile channel characterization and modeling and future mobile broadband systems. He was or is involved in European projects and networks of excellence COST 273, IST/FLOWS, ICT/4WARD, ICT/EARTH, ICT/LEXNET, NEWCOM, and NEWCOM++. He was the Task Leader of Energy Efficiency in Transmission Techniques (EARTH) and Dissemination and Standardization (LEXNET) workgroups. He has authored papers in national and international conferences and journals, for which he has also served as a reviewer and board member. He was Secretary of the IEEE ComSoc Portuguese Chapter.

SŁAWOMIR J. AMBROZIAK (Senior Member, IEEE) was born in Poland, in 1982. He received the M.Sc., Ph.D., and D.Sc. degrees in radio communication from the Gdańsk University of Technology (GUT), Poland, in 2008, 2013, and 2020, respectively. Since 2008, he has been with the Department of Radio communication Systems and Networks, GUT, as Research Assistant (2008–2013), as an Assistant Professor (2013–2020), and has been a Associate Professor, since 2020. He is an author or coauthor of many publications, including book chapters, articles, reports, and papers presented during international and domestic conferences. He has participated and still participates in several projects related to special application of wireless techniques as well as two COST Actions (IC1004 and CA15104). His main scope of research is radio channel modelling in body area networks. In addition, his research interests include wireless communication and radio wave propagation. He is a member of the Gdansk Scientific Society. He is also a member of the Board of the Working Group on Propagation of the European Association on Antennas and Propagation (EurAAP), the Management Committee Substitute Member of the COST CA15104 Action and Chair of the Sub Working Group Internet-of-Things for Health within this action, and the Vice-Chair of the Commission-F of the Polish National Committee of URSI. He was a recipient of the Young Scientists Awards of URSI, in 2016 and 2011, the Eighth International Conference on Wireless and Mobile Communications Best Paper Award, in 2012, and many domestic awards.

LUIS M. CORREIA (Senior Member, IEEE) was born in Portugal, in 1958. He received the Ph.D. degree in electrical and computer engineering from the University of Lisbon (IST), in 1991, where he is currently a Professor in telecommunications, with his work focused on wireless/mobile communications in the areas of propagation, channel characterization, radio networks, traffic, and applications, with the research activities developed in the INESC-ID institute. He has acted as a Consultant for the Portuguese telecommunications operators and regulator, besides other public and private entities, and has been in the Board of Directors of a telecommunications company. Besides being responsible for research projects at the national level, he has participated in 31 projects within European frameworks, having coordinated six and taken leadership responsibilities at various levels in many others. He has supervised more than 200 M.Sc./Ph.D. students, having edited six books, contribute to European strategic documents, and has authored more than 500 papers in international and national journals and conferences, for which he also served as a reviewer, editor, and board member. Internationally, he was a part of 36 Ph.D. juries, and 63 research projects and institutions evaluation committees for funding agencies in 12 countries and the European Commission. He has been the Chairman of Conference, of the Technical Programme Committee, and of the Steering Committee of various major conferences, besides other several duties. He was a National Delegate to the COST Domain Committee on ICT. He was active in the European Net!Works platform by being an elected member of its Expert Advisory Group and of its Steering Board, and the Chairman of its Working Group on Applications, and was also elected to the European 5G PPP Association. He has launched and served as the Chairman of the IEEE Communications Society Portugal Chapter.

• • •